The Formation and Recombination Kinetics of Positively Charged Poly(phenylene vinylene) Chains in Pulse-Irradiated Dilute Solutions

Ferdinand C. Grozema, Romano J. O. M. Hoofman, Luis P. Candeias, Matthijs P. de Haas, John M. Warman, and Laurens D. A. Siebbeles*

Radiation Chemistry Department, IRI, Delft University of Technology, Mekelweg 15, 2629 JB Delft, The Netherlands

Received: November 7, 2002; In Final Form: February 25, 2003

In this paper, we describe how we derive the mobility of positive charges ("holes") along isolated conjugated polymer chains from the results of pulse-radiolysis time-resolved microwave conductivity (PR-TRMC) experiments on dilute polymer solutions. The method is illustrated with results for oxygen-saturated, benzene solutions of the well-known poly(phenylene vinylene) derivative, MEH−PPV with an average chain length of 800 monomer units. Nanosecond pulsed irradiation results initially in ionization of the solvent with the formation of excess electrons and benzene radical cations, Bz^+. The former rapidly (<1 ns) undergo attachment to O_2 to form O_2^- with a rate constant of 1.5×10^{11} M^{-1} s^{-1}. The Bz^+ ions diffuse through the solvent and react with the (lower ionization potential) polymer chains via electron abstraction forming holes on the polymer backbone. This is accompanied by a large increase in the conductivity of the solution after the pulse, demonstrating that the mobility of holes on the polymer chains is very much larger than the mobility, via molecular diffusion, of Bz^+ ions in the solvent. To describe the after-pulse growth in conductivity, a large effective reaction radius, R_{eff}, of ca. 400 Å is required for the diffusion-controlled reaction of Bz^+ with MEH−PPV chains. This requires taking into account the time-dependent term in the rate coefficient. The value of R_{eff} is compared with theoretical predictions for the reaction of a small entity with a 1-D linear or a 3-D cubic array of 800 reactive moieties. The conclusion that individual polymer chains in solution must have a very open structure with a large persistence length is in agreement with the results of previous static and dynamic light-scattering studies. The conductivity eventually decays because of the recombination of the positively charged polymer chains with negative counterions (O_2^-) with a rate coefficient of 1.2×10^{11} M^{-1} s^{-1}, which is somewhat slower than predicted by the Debije equation. No evidence could be found for first-order trapping of the mobile positive charge on the polymer chains prior to recombination. The pseudo-one-dimensional mobility of holes along the polymer backbone derived from the absolute magnitude of the conductivity transients is 0.46 cm^2 V^{-1} s^{-1}.

Introduction

The mechanism of charge transport in conjugated polymers is a topic of considerable interest since these materials are being considered for application in electronic devices.[1−6] Examples of such devices include field effect transistors (FETs), light-emitting diodes (LEDs), and photovoltaic cells. The performance characteristics (e.g., switching times and maximum current) of these devices are critically dependent on the mobility of the charge carriers. We have recently shown that it is possible to measure the mobility of charges along isolated chains of conjugated polymers in solution using the pulse-radiolysis time-resolved microwave conductivity technique (PR-TRMC).[7,8] The mobility of charge along an isolated polymer chain in solution cannot be compared directly with charge carrier mobilities in the corresponding bulk solid—the state in which these materials are used in devices. In the solid, charge transport can occur via interchain as well as intrachain mechanisms. In addition, the static and dynamic disorder within the backbone of the polymer is expected to be quite different in the two phases.

Measurements of charge transport on isolated chains do, however, provide unique data on charge transport along molecular wires—information which is useful for gaining an insight into the relation between the molecular structure of conjugated polymers and their conductive properties. The results are especially interesting because isolated polymer chains are also tractable for theoretical treatments that take the inherently disordered nature of polymers into account.[9] Moreover, direct measurements of the *intra*-molecular mobility for different polymers can present a useful guideline for the design of molecular wires with transport properties that meet the requirements of nanoscale electronics.

Recently, we have reported mobilities of positive charges along isolated polymer chains in benzene solution for a variety of σ- and π-conjugated polymers.[7] For both types of polymer, the mobility depended strongly on the molecular structure of the polymer backbone and on the nature of the side chains.

It is the purpose of this paper to give a detailed account of the kinetic fitting procedure that was used to obtain the charge carrier mobility from the time-resolved microwave conductivity measurements, using a poly(phenylene vinylene) derivative, MEH−PPV (see Figure 1) as an example. This requires a detailed description of the kinetics of formation and decay of the positively charged polymer chains. Both the formation and decay involve diffusion-limited reactions between a small mobile

* Corresponding author. E-mail: siebbel@iri.tudelft.nl.

10.1021/jp022379c CCC: $25.00
Published on Web 07/11/2003

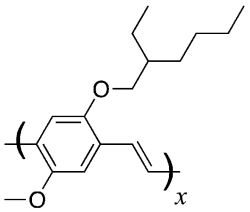

Figure 1. Molecular structure of MEH−PPV.

entity and a large, relatively immobile, polymer chain. The complex kinetics of such reactions are not only relevant for the particular problem that is addressed in this work but are of general importance.[10] Examples of diffusion-limited reactions of the type discussed here include fluorescence quenching,[11,12] reaction of small reactive species with polymers,[13] and the binding of a small substrate to the catalytic site of an enzyme.[14] There have been many theoretical studies of such processes, using both analytical[15−22] and numerical methods.[20−22]

We first discuss the experimental procedures used to measure the radiation-induced conductivity and the radiolytic processes which occur. We then describe the analysis of the kinetics of the diffusion-controlled formation and decay reactions of positively charged polymer chains and the procedure used to fit the conductivity transients observed.

Experimental Details

The chemical structure of the poly(phenylene vinylene) derivative studied in this work, poly(2-methoxy-5-[2′-ethyl-hexyloxy]-phenylenevinylene), MEH−PPV, is shown in Figure 1. According to gel permeation chromatography (GPC) measurements, the polymer has an estimated number-averaged molecular weight, M_n, of 200 ± 100 kDa, which corresponds to 800 ± 400 monomer units. The alkoxy side chains make it possible to dissolve the polymer in a variety of organic solvents. Dilute solutions in benzene (Merck UV spectroscopic grade) were freshly prepared before each experiment. The concentrations ranged from 0.2 mM to 1.0 mM in monomer units. This corresponds to polymer chain concentrations from 0.25 to 1.25 μM for a molecular weight of 200 kDa. No indication of polymer aggregation was observed. The solutions were bubbled with oxygen for at least 10 min before transferring them to a vacuum-tight microwave cell. The O_2 concentration in a saturated solution is ca. 12 mM.

A schematic drawing of the experimental setup used for the experiments described in this paper is shown in Figure 2. Excess charge carriers were produced in the solution by pulsed irradiation with 3 MeV electrons from a Van de Graaff accelerator using pulse durations from 2 to 50 ns. Electrons with an energy of 3 MeV have a penetration depth of 15 mm in benzene, which is much larger than the 3.55-mm thickness of the microwave cell that contains the polymer solution. Energy deposition by the electron beam as it traverses the sample is therefore close to uniform. In a multicomponent medium, energy is initially distributed between the individual components according to their fractional contribution to the overall electron density. In the solutions used in the present work, the contribution of the polymer to the electron density was less than 0.1% even for the highest polymer concentration used. Therefore, energy is initially deposited almost exclusively in the benzene solvent.

The initial concentration of charge carriers is proportional to the amount of energy deposited per unit volume, which is the radiation dose, D_v (Jm^{-3}). The dose was calibrated using thin film radiochromic dosimeters (Far West Technology) and was

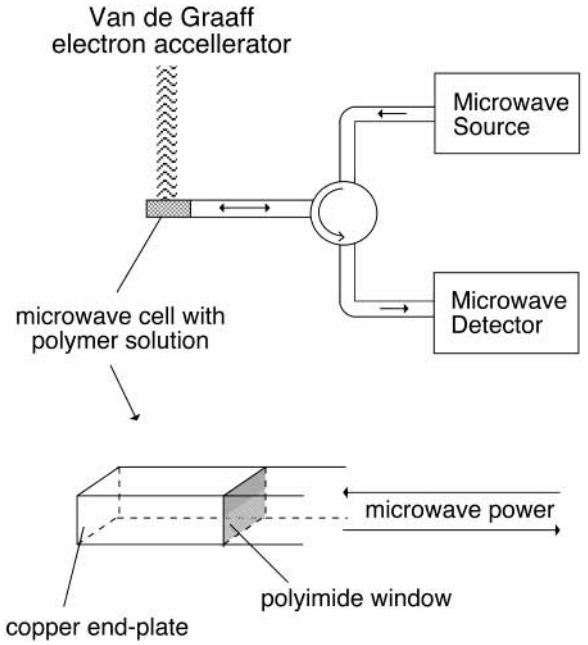

Figure 2. Schematic drawing of the PR-TRMC setup.

530 Jm^{-3} per nanocoulomb beam charge. The integrated beam charge per pulse, Q (nC), was routinely measured for each pulse. The concentration in moles per liter of a radiolytic product X formed within a pulse is given by

$$[\mathrm{X}] = \frac{530\,Q}{6.02 \times 10^{26} e E_{\mathrm{X}}} \qquad (1)$$

with E_X the average energy in eV absorbed per product X formed. As an example, for a 10-ns pulse Q is ca. 40 nC. Taking this together with the value of 1900 eV for the average energy to form one free ion pair in benzene[23,24] results in an estimated concentration of ion pairs formed of 0.12 μM.

Irradiation of benzene leads to the formation of radiochemical products, such as biphenyl, which can react with the initially formed excess electrons and benzene radical cations.[25] The accumulated irradiation dose used in the experiments described in the following sections was therefore kept sufficiently low that such radiolytic products did not affect the conductivity transients measured. No change in the magnitude or shape of a conductivity transient for a given solution was observed for the total accumulated dose used in a series of measurements on a single solution. From separate, steady-state radiolysis experiments it has been found that a total dose of more than an order of magnitude larger than the doses used in the present pulsed experiments is required to induce a detectable change in the optical absorption of oxygen saturated MEH−PPV solutions.

The radiation-induced conductivity in the solutions was measured using the time-resolved microwave conductivity (TRMC) technique.[26−28] The microwave system is constructed of rectangular waveguide with internal cross section 7.1 × 3.55 mm^2. Microwave frequencies in the Ka-band (26.5−40 GHz) were used, corresponding to a reciprocal radian frequency of ca. 5 ps. The average microwave power level was 100 mW which corresponds to an electric field amplitude within the cell of ca. 10 V cm^{-1}. The microwave cell containing the polymer solution is closed at one end with a metal plate and at the other end with a vacuum-tight polyimide window, see Figure 2. The probing microwaves are reflected at the metal end plate and form a standing wave pattern in the cell.

Changes in the conductivity inside the cell upon pulsed irradiation were monitored as changes in the microwave power reflected by the cell. The output of the microwave detector diode was monitored using either a linear time base with a Tektronix TDS 680B two-channel digital real-time oscilloscope or a logarithmic time base using a Sony/Tektronix RTD 710 digitizer. Using the latter combination, conductivity transients could be monitored from 10 ns to 1 ms using a single accelerator pulse.

The change in the microwave power reflected by the cell, ΔP_R, is directly proportional to the change in the conductivity of the sample, $\Delta\sigma$, for small changes in the conductivity,

$$\frac{\Delta P_R}{P_R} = A\Delta\sigma \tag{2}$$

The sensitivity factor, A, can be calculated from the geometric and dielectric properties of the sample and the microwave frequency used as described previously.[26−28] The radiation-induced conductivity is related to the mobility of the charge carriers formed, μ_i, according to

$$\Delta\sigma(t) = e\sum_i N_i(t)\mu_i \tag{3}$$

In eq 3, $N_i(t)$ is the number density of charge carriers of type i existing at time t and e is the elementary charge. The radiation-induced conductivity is usually given as the dose-normalized quantity $\Delta\sigma/D_v$ ($Sm^2\ J^{-1}$).

Results and Discussion

As mentioned in the Introduction, it is the purpose of this paper to present a detailed description of the method of data analysis used to derive the mobilities of charge carriers on conjugated polymer chains from TRMC measurements on pulse-irradiated dilute polymer solutions.[7,8] The emphasis is therefore more on the reaction mechanisms and kinetics which underlie the growth and decay of the conductivity after the pulse rather than on the absolute value of the mobility derived, which has been published previously.[7,8] The method of data treatment and the type of information obtained are illustrated by measurements on dilute, oxygen-saturated solutions of the conjugated polymer MEH−PPV. As pointed out in the Experimental Section, energy from the incident 3 MeV electrons will be transferred initially almost exclusively to molecules of the solvent. Because of this, we first discuss the radiolytic processes occurring in the solutions after pulsed irradiation.

Radiolytic Processes. Radiolysis of benzene results initially in ionization and excitation of individual molecules of the medium leading to the formation of benzene radical cations, Bz^+, excess electrons, e^-, and excited states, represented by Bz*. In the present conductivity study, we are principally interested in the charged species since these are specifically monitored using the TRMC technique. These are initially formed as coulomb-correlated pairs $\{Bz^+ + e^-\}$ with an average separation distance $R_\pm$ of approximately 50 Å,[29] which is considerably less than the Onsager escape distance, R_c.

$$Bz \rightsquigarrow \{Bz^+ + e^-\} \tag{A}$$

R_c is the distance at which the coulomb energy is equal to the characteristic thermal energy k_BT (ca. 0.025 eV at room temperature) and is given in terms of the relative dielectric constant, ϵ, by

$$R_c = \frac{e^2}{4\pi\epsilon\epsilon_0 k_B T} \tag{4}$$

with ϵ_0 the permittivity of vacuum, e the elementary charge, k_B the Boltzmann constant, and T the temperature. For liquid benzene $\epsilon = 2.28$ and $R_c = 250$ Å. Because $R_\pm$ is much smaller than R_c at room temperature, a large fraction of the initial ionization events are followed by rapid, "geminate" charge recombination on a subnanosecond time scale.[27]

$$\{Bz^+ + e^-\} \rightarrow Bz^* \tag{B}$$

Only a small fraction, F_{fp}, of the initially formed pairs is capable of undergoing diffusional escape resulting in the formation of relatively long-lived, homogeneously distributed "free" ions.

$$\{Bz^+ + e^-\} \xrightarrow{F_{fp}} Bz^+ + e^- \tag{C}$$

The yield of free ions in benzene at room temperature has been determined, in DC conductivity experiments, to be 0.053 per 100 eV absorbed.[23,24] This corresponds to an average energy for the formation of a free ion pair, E_{fp}, of 1900 eV and to a value of F_{fp} of approximately 1%. It is this small escaped fraction that is relevant in the present work since these free ions can diffuse throughout the solvent and react with dissolved solutes. The geminately recombining ions, on the other hand, will have decayed well within the shortest time scale of a few nanoseconds prevailing in the present experiments.

The conductivity resulting on nanosecond pulse-radiolysis of pure benzene is given by

$$\Delta\sigma = eN_{fp}[\mu(e^-) + \mu(Bz^+)] \tag{5}$$

with $\mu(e^-)$ and $\mu(Bz^+)$ the mobility of the excess electron and solvent radical cation, respectively, and N_{fp} the concentration of free ions. If no decay of free ions occurs during the pulse, then the end-of-pulse value of N_{fp} for a dose in the pulse of D_v in Jm^{-3} will be

$$N_{fp}(0) = \frac{D_v}{E_{fp}} \tag{6}$$

Substitution for $N_{fp}(0)$ from eq 6 in eq 5 and rearrangement gives for the experimentally measurable quantity $[\Delta\sigma/D_v]_0$

$$[\Delta\sigma/D_v]_0 = \frac{e[\mu(e^-) + \mu(Bz^+)]}{E_{fp}} \tag{7}$$

DC conductivity experiments have shown the excess electron to be the major charge carrier in benzene with a mobility of 0.13 $cm^2\ V^{-1}\ s^{-1}$ at room temperature.[23,30] A mobility of 1.2×10^{-3} $cm^2\ V^{-1}\ s^{-1}$ for Bz^+ has been estimated previously from PR-TRMC measurements using an X-band resonant cavity. This value is close to that which would be expected for diffusive molecular motion within a liquid of viscosity 0.65 cP, that is, it corresponds to a diffusion coefficient, D, of 3×10^{-5} $cm^2\ s^{-1}$ according to the Einstein relationship

$$D = \frac{\mu k_B T}{e} \tag{8}$$

Substituting the above mobilities and the value of E_{fp} in eq 7 yields a predicted value of $[\Delta\sigma/D_v]_0$ for pure benzene of 6.9×10^{-9} $Sm^2\ J^{-1}$.

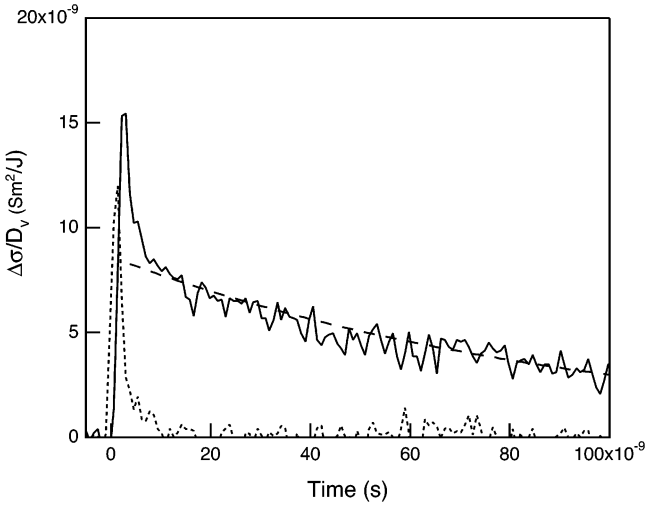

Figure 3. Radiation-induced conductivity in neat benzene (solid line) and oxygen-saturated benzene (dotted line) using a 2-ns electron pulse. The dashed line is an exponential fit to the transient for neat benzene.

A dose-normalized TRMC transient obtained on pulse-radiolysis of pure benzene using a 2-ns pulse is shown in Figure 3. The initial rapid decay of the conductivity during the first 2−5 ns is attributed to a tail of the geminately recombining ion pairs. The conductivity at longer times is due to free ion pairs that have escaped from geminate recombination. The first half-life of the decay of this conductivity component, as indicated by the dashed line in Figure 3, is ca. 70 ns. Since this is considerably longer than the 2-ns pulse length used, we conclude that only a small fraction of the free ions will have recombined within the pulse. The end-of-pulse value of $\Delta\sigma/D_v$ should therefore be close to the value of $[\Delta\sigma/D_v]_0$ given above. The value found by extrapolation of the relatively slowly decaying conductivity component to the end of the pulse is 8.0×10^{-9} $Sm^2\ J^{-1}$. This is approximately 15% higher than the value of 6.9×10^{-9} $Sm^2\ J^{-1}$ predicted on the basis of previous DC measurements. In view of the very different experimental techniques used to derive $[\Delta\sigma/D_v]_0$, we consider the agreement to be reasonable. The larger value of $[\Delta\sigma/D_v]_0$ found in the present work could be due to a higher mobility or a larger free-ion yield (lower value of E_{fp}) than measured in the DC experiments. Since the value of $E_{fp} = 1900$ eV has been independently determined by two different groups, we have consistently used this value to calculate the concentration of free ions formed. If the value of E_{fp} is in fact 15% lower, then the values of the polymer hole mobility calculated on the basis of $E_{fp} = 1900$ eV would be approximately 15% too high.

Since the electron is by far the most mobile charge carrier in pure benzene, the after-pulse decay of the conductivity reflects mainly the decay of this species. In the absence of electron-attaching impurities or additives, decay will occur by homogeneous charge recombination according to

$$Bz^+ + e^- \xrightarrow{k_D} Bz \qquad (D)$$

In molecular liquids, the reaction coefficient for charge recombination, k_r, is given in general by the Debye relation[31]

$$k_r = \frac{e[\mu_+ + \mu_-]}{\epsilon\epsilon_0} = 4\pi R_c[D_+ + D_-] \qquad (9)$$

with μ_+ and μ_- the mobilities of the recombining ions and D_+ and D_- the corresponding diffusion constants (see eq 8). The resulting time dependence of the free-ion concentration after the pulse should then be given by

$$\frac{N_{fp}(t)}{N_{fp}(0)} = \frac{1}{1 + N_{fp}(0)k_r t} \qquad (10)$$

The first half-life due to recombination alone, τ_r, is therefore

$$\tau_r = \frac{1}{N_{fp}(0)k_r} \qquad (11)$$

Substituting in eq 11 for $N_{fp}(0)$ from eq 6 and for k_r from eq 9 leads to the following expression:

$$\tau_r = \frac{E_{fp}\epsilon\epsilon_0}{eD_v[\mu_+ + \mu_-]} \qquad (12)$$

Taking the known values of E_{fp}, ϵ, and $[\mu_+ + \mu_-]$ corresponding to reaction D together with the dose of $4.2 \cdot 10^3$ Jm^{-3} used for the transient in Figure 3 results in a predicted value for τ_r of ca. 700 ns.

This half-life estimated for recombination alone is substantially longer than the actual half-life of 70 ns derived from the transient in Figure 3. An additional decay channel to D for electrons must therefore be operative. This is attributed to the occurrence of electron attachment to spurious impurities, I_e, in the nominally pure solvent.

$$e^- + I_e \xrightarrow{k_E} I_e^- \qquad (E)$$

For an electron mobility of 0.13 $cm^2\ V^{-1}\ s^{-1}$, the rate constant for reaction (E) could be as high as 3×10^{12} $M^{-1}\ s^{-1}$.[27] An impurity concentration of as little as 5 micromolar (corresponding to only ca. 1 ppm) would therefore be sufficient to result in the half-life of 70 ns found.

Neat benzene may also contain small concentrations of spurious impurities which can scavenge the initially formed Bz^+ radical cations.

$$Bz^+ + I_h \xrightarrow{k_F} Bz + I_h^+ \qquad (F)$$

Because of the much lower diffusion coefficient of Bz^+, the rate coefficient for this reaction will, however, be much smaller than that for reaction E and close to the value of 1×10^{10} $M^{-1}\ s^{-1}$ expected for a diffusion-controlled reaction between molecular species.

As pointed out above, only small amounts of electron-attaching compounds are sufficient to considerably shorten the electron lifetime. By deliberately adding such an electron "scavenger", the conductivity signal due to excess electrons can be almost completely suppressed. This is shown in Figure 3 by the TRMC transient for an oxygen-saturated (12 mM) solution in which electron attachment occurs via G.

$$e^- + O_2 \xrightarrow{k_G} O_2^- \qquad (G)$$

From the decay of the conductivity in solutions containing a lower concentration of oxygen, we have determined the rate constant for electron scavenging by O_2 to be $k_G = 1.5 \times 10^{11}$ $M^{-1}\ s^{-1}$. For an O_2-saturated solution, the concentration is therefore high enough to reduce the electron lifetime to less than a nanosecond as shown in Figure 3.

In the present work, we have used oxygen as an electron scavenger rather than CCl_4 which was used in a previously

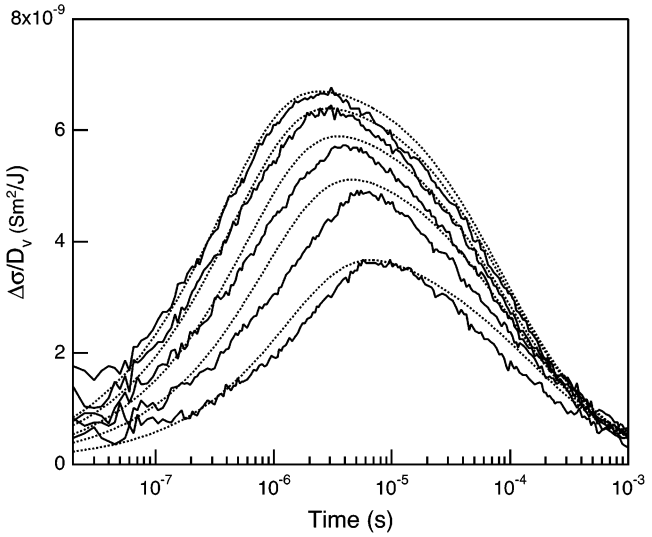

Figure 4. Dose-normalized radiation-induced conductivity in benzene solutions of MEH−PPV for different concentrations obtained using a 10-ns pulse. From top to bottom: 1.25 μM, 1.0 μM, 0.75 μM, 0.5 μM, and 0.25 μM (polymer concentrations). The dotted lines represent kinetic fits for which all parameters were held constant apart from the polymer concentration.

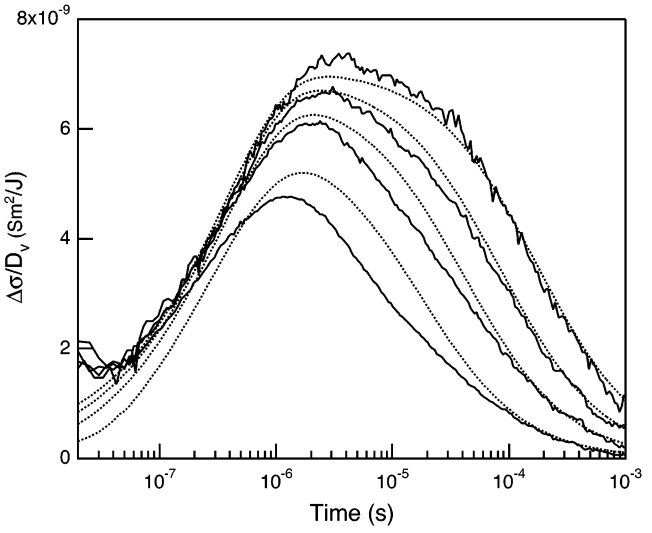

Figure 5. Dose-normalized radiation-induced conductivity in benzene solutions of MEH−PPV for different pulse durations, from top to bottom: 5, 10, 20, and 50 ns. The dotted lines represent kinetic fits for which all parameters were held constant apart from the concentration of ion pairs formed in the pulse.

reported study.[8] This was motivated by the fact that electron attachment to O_2 is nondissociative and does not produce a strongly oxidizing free-radical species such as CCl_3^- on pulse-radiolysis which could possibly lead to subsequent oxidation of the polymer.

When using O_2-saturated solutions, care has to be taken that the sample is not exposed for extensive periods of time to light. This was achieved in the present work by transferring the solutions to the microwave cell within a few minutes after saturation with oxygen. We have previously carried out a quantitative study of the UV photo-oxidative degradation of MEH−PPV in benzene solution[32] and found a 10% reduction in the microwave photoconductivity for a total absorbed dose of UV radiation of ca. 20 J/cm^3. An exposure of many hours would be required to reach this level of photodegradation under normal laboratory lighting conditions. As far as radiolytic degradation goes, we have observed no significant change in the temporal form or absolute magnitude of the conductivity transients during the course of a series of experiments. Deliberate exposure of O_2-saturated MEH−PPV solutions to large doses of ionizing radiation in a Cobalt-60 source have shown only small, <10%, changes in the optical absorption for doses 10 times the total accumulated dose used in the present pulse-radiolysis experiments.

Benzene radical cations do not react with oxygen but diffuse through the solvent and eventually undergo charge transfer to the conjugated polymer chains (reaction H), which have a lower ionization potential.

$$Bz^+ + PPV \xrightarrow{k_H} Bz + PPV^+ \qquad (H)$$

Figure 4 shows the time dependence of the microwave conductivity after pulsed irradiation for polymer concentrations ranging from 0.25 μM to 1.25 μM. The conductivity is seen to increase initially after the pulse on a time scale of hundreds to thousands of nanoseconds. As is evident from Figure 4, this after-pulse growth becomes faster with increasing polymer concentration, in accordance with expectations based on reaction H as the underlying source. These results provide immediate qualitative evidence that the mobility of positive charges on MEH−PPV chains is considerably higher than that of Bz^+ ions in benzene. The large increase in mobility is due to motion of charge along the polymer chain rather than diffusional motion of the polymer chains as a whole.

The conductivity eventually decays on a time scale of tens to hundreds of microseconds as shown in Figures 4 and 5. In Figure 5, the time scale of the decay of the conductivity is seen to become shorter as the pulse duration increases, that is, as the concentration of ion pairs formed in the pulse is increased. Accordingly, we attribute this decay to second-order charge recombination of PPV^+ with O_2^-.

$$PPV^+ + O_2^- \xrightarrow{k_I} PPV + O_2 \qquad (I)$$

To obtain the absolute value for the mobility, the concentration of charged polymer chains in the solution must be known as a function of time. This can be obtained from a kinetic scheme that includes all the relevant reactions that occur upon pulsed irradiation of the polymer solutions. The rate coefficients and mobilities that are unknown are adjusted such that an optimal correspondence between the calculated conductivity transients and the experimental data in Figures 4 and 5 is obtained. This fitting procedure and the resulting rate coefficients and mobility are discussed in the following sections.

Reaction Kinetics. The kinetics of the reactions A−I can be described by a set of differential equations for the formation and decay of the five relevant species (e^-, Bz^+, PPV^+, O_2^-, I_h^+). Freely diffusing Bz^+ and e^- are formed during the electron pulse by processes A and C. As discussed above the geminate recombination process, reaction B takes place on a time scale of less than a nanosecond, whereas the reactions that we are mainly interested in occur on time scales of tens of nanoseconds or longer. Therefore, only the "free" ions that escape from geminate recombination by reaction C are considered in the kinetic analysis.

Since the time profile of the Van de Graaff electron pulses is close to rectangular with rise and fall times of ca. 100 ps, the formation of free ions during the pulse can be well described by

$$\frac{dN_{fp}}{dt} = \frac{D_v}{E_{fp}\Delta\tau} \qquad (0 < t < \Delta\tau) \tag{13}$$

where $\Delta\tau$ is the pulse duration. This results in a linear increase of $[Bz^+]$ and $[e^-]$ with time during the pulse. The decay of excess electrons occurs mainly by reaction with the dissolved oxygen:

$$\frac{d[e^-]}{dt} = -k_G[e^-][O_2] \tag{14}$$

Reaction of excess electrons via D or E is insignificant compared to the rate of attachment to O_2.

For the benzene radical cations, there are four possible decay pathways: homogeneous recombination with e^- (reaction D), reaction with MEH−PPV (reaction H), reaction with hole-scavenging impurities (reaction F), and finally charge recombination with O_2^- (reaction J).

$$Bz^+ + O_2^- \xrightarrow{k_J} Bz + O_2 \tag{J}$$

These decay pathways lead to the following differential equation for the decay of Bz^+:

$$\frac{d[Bz^+]}{dt} = -k_D[e^-][Bz^+] - k_F[Bz^+][I_h] - k_H[Bz^+][PPV] - k_J[Bz^+][O_2^-] \tag{15}$$

Positive charges can become trapped at hole-scavenging impurities, denoted by I_h, by reaction F and can subsequently recombine by reaction with O_2^- via reaction K,

$$I_h^+ + O_2^- \xrightarrow{k_K} I_h + O_2 \tag{K}$$

which gives for the evolution of $[I_h^+]$ with time:

$$\frac{d[I^+_h]}{dt} = +k_F[I_h][Bz^+] - k_K[I^+_h][O^-_2] \tag{16}$$

PPV^+ is formed by charge transfer from Bz^+ and decays by charge recombination with O_2^-:

$$\frac{d[PPV^+]}{dt} = +k_H[Bz^+][PPV] - k_I[O_2^-][PPV^+] \tag{17}$$

The charge recombination reaction of PPV^+ with e^- can be neglected since the fraction of e^- that has not yet reacted with O_2 on the time scale on which PPV^+ is formed is negligible.

The formation of O_2^- occurs via reaction G while its decay is due to charge recombination with Bz^+, PPV^+, and I_h^+.

$$\frac{d[O_2^-]}{dt} = +k_G[e^-][O_2] - k_J[Bz^+][O_2^-] - k_I[O_2^-][PPV^+] - k_K[I_h^+][O_2^-] \tag{18}$$

The concentrations of charged species as a function of time and the mobility of the species together determine the conductivity of the solution according to eq 3. Fits to the experimental data in Figures 4 and 5 were obtained by numerically integrating the differential eqs 13−18 using the Runge−Kutta method. In the fitting procedure, the rate coefficients of reactions H and I are the variables which mainly determine the shape of the radiation-induced conductivity transients, while the charge mobility on MEH−PPV mainly determines the absolute magnitude of the transients. In the following section, we discuss the values of the rate coefficients and mobilities used in this fitting procedure with particular attention given to the (possible) time dependence of the former.

TABLE 1: Mobility Values Used in the Fitting Procedure

ion	mobility (cm^2/Vs)	comments
e^-	0.13	from refs 28 and 30
Bz^+	0.0012	from ref 33
O_2^-	0.0010	from ref 34[a]
I_h^+	0.0012	assumed $\approx\mu(Bz^+)$
P^+	0.000004	from ref 39[c]
h^+/P	0.46 (1 − D)[b]	this work

[a] From $\mu(O_2^-)$ determined in liquid cyclohexane and iso-octane in ref 33 adjusted to the viscosity of liquid benzene. [b] Three times the isotropic value of 0.153 $cm^2\ V^{-1}\ s^{-1}$ used to fit the experimental conductivity transients. [c] From D(P) determined by dynamic light scattering.

Mobilities and Rate Coefficients (Small Molecular Species). Numerical integration of the differential rate equations given in the previous section and calculation of the time dependence of the conductivity requires, as input, values of the mobilities of the charged species listed in Table 1 and the rate coefficients of the reactions listed in Table 2. For the small (as opposed to polymeric) molecular species, these parameters are known from previous work or have been determined in separate experiments as mentioned earlier in this article. Summarizing the mobility values: $\mu(e^-) = 0.13\ cm^2\ V^{-1}\ s^{-1}$ has been determined by time-of-flight measurements;[23,30] $\mu(Bz^+) \approx 1.2 \times 10^{-3}\ cm^2\ V^{-1}\ s^{-1}$ was obtained from previously unreported PR-TRMC measurements on electron-scavenged benzene solutions using a more sensitive X-band resonant cavity method;[33] $\mu(I_h^+) \approx \mu(Bz^+)$ is a reasonable assumption since $\mu(Bz^+)$ is close to the value expected for molecular diffusion in a liquid with the viscosity of benzene (0.65 cP); $\mu(O_2^-) \approx 1.0 \times 10^{-3}\ cm^2\ V^{-1}\ s^{-1}$ was estimated by interpolation between the values of $\mu(O_2^-)$ determined by time-of-flight measurements in the hydrocarbon solvents cyclohexane ($\eta = 1.0$ cP) and isooctane ($\eta = 0.35$ cP).[34]

The following rate coefficients were taken as fixed parameters: $k_E = 1.0 \times 10^7\ s^{-1}$ derived from the excess electron decay in nominally pure, deaerated benzene; $k_G = 1.5 \times 10^{11}\ M^{-1}\ s^{-1}$ from the excess electron decay in air-saturated benzene; k_D, k_J, and k_K were calculated using the Debije relation for diffusion-controlled recombination (eq 9) with the relevant mobility values taken from Table 1 and $R_C = 250$ Å. Inclusion of reaction F, with a rate of $1.0 \times 10^5\ s^{-1}$, was necessary to provide a satisfactory description of the concentration dependence. This reaction has, however, little influence on the temporal form of the calculated transients.

A factor which must be considered in the calculations is the possibility that the rate coefficients are time dependent on the time scale of the measurements. Smoluchowski[16] has shown that the rate coefficient for a diffusion-controlled reaction between two small (spherical) reactants i and j should be time-dependent according to

$$k_{ij}(t) = 4\pi R_{ij} D_{ij}\left[1 + \frac{R_{ij}}{\sqrt{(\pi D_{ij} t)}}\right] \tag{19}$$

In eq 19, R_{ij} is the distance apart at which reaction is considered to irreversibly occur (the "reaction radius") and D_{ij} ($=D_i + D_j$) is the sum of the diffusion coefficients of the reactants. From eq 19 it can be seen that for times much longer than $R^2_{ij}/\pi D_{ij}$,

TABLE 2: Rate Coefficients Used in the Fitting Procedure

reaction	reactants	rate coefficient	comments
D	$Bz^+ + e^-$	6.2×10^{13} M^{-1} s^{-1}	$k_D = [\mu(Bz^+) + \mu(e^-)]e/\epsilon\epsilon_0$[a]
E	$e^- + I_e$	1.0×10^7 s^{-1}	this work, electron decay in "pure" benzene
F	$Bz^+ + I_h$	1.0×10^5 s^{-1}	this work, from fits for PPV solutions
G	$e^- + O_2$	1.5×10^{11} M^{-1} s^{-1}	this work, electron decay in benzene + O_2 soln
H	$Bz^+ + PPV$	eq 24	$D(Bz^+) = 3 \times 10^{-5}$, $R_{eff} = 360$ Å
I	$PPV^+ + O_2^-$	1.2×10^{11} M^{-1} s^{-1}	this work, from fits for PPV solutions
J	$Bz^+ + O_2^-$	1.2×10^{12} M^{-1} s^{-1}	$k_J = [\mu(Bz^+) + \mu(O_2^-)]e/\epsilon\epsilon_0$[a]
K	$I_h^+ + O_2^-$	1.2×10^{12} M^{-1} s^{-1}	$k_K = k_J$

[a] The Debye relation for diffusion-controlled charge recombination; eq 9 in text.

the time-dependent term becomes negligible and reaction proceeds with the limiting, time-independent rate constant k_{ij}.

$$k_{ij} = 4\pi R_{ij} D_{ij} \tag{20}$$

For the contribution of the time-dependent term to be less than 10%, the following inequality for the time scale on which reaction occurs must be fulfilled.

$$t > \frac{10R^2_{ij}}{\pi D_{ij}} \tag{21}$$

For reactions between an ion and a neutral molecule, values of R_{ij} about 5 Å are found for species with dimensions of a few Ångstroms.[35] The rate coefficients for such reactions can therefore be taken to be constant for times longer than $8 \times 10^{-15}/D_{ij}$ seconds, for D_{ij} in units of cm^2 s^{-1}. For excess electron reactions in benzene, D_{ij} is dominated by the high electron diffusion coefficient of 3.3×10^{-3} cm^2 s^{-1}. The values of k_E and k_G may therefore be considered to be time-independent for times in excess of approximately 2 ps, a condition which is amply fulfilled in the present experiments. For reaction F, the value of D_{ij} will be approximately 5×10^{-5} cm^2 s^{-1} and the assumption of a constant value of k_F will therefore be valid for times longer than ca. 200 ps. Since this reaction is operative on the same time scale as the after-pulse growth of the conductivity, that is, several hundred nanoseconds, condition 21 will also be fulfilled for reaction F.

The recombination reactions D, J, and K between small charged species have an effective value of R_{ij} equal to the Onsager radius R_C (see eq 4) which is 250 Å for benzene. This results in a time of $2 \times 10^{-11}/D_{ij}$ seconds above which the time-independent value of the rate coefficient given by the Debye expression (eq 19) can be assumed to apply. Taking the diffusion coefficients corresponding to the mobilities given in Table 1 results in limiting times of 6 ns for reaction D and ca. 400 ns for reactions J and K. The former limit is considerably shorter than the decay time of electrons in pure benzene and the latter is much shorter than the time scale of many microseconds on which recombination of molecular ions occurs, as indicated by the decay of the conductivity transients in the polymer solutions. The assumption of a constant rate coefficient for the recombination reactions D, J, and K, as given by eq 19, is therefore justified.

Mobilities and Rate Coefficients (Polymeric Species). As mentioned previously, three parameters have a dominant influence on the temporal form and absolute magnitude of the conductivity transients in the present experiments. These are (1) the rate coefficient for charge transfer from Bz^+ to the polymer, k_H, which governs the after-pulse growth of the conductivity, (2) the rate coefficient for neutralization of the charged polymer chains by O_2^-, k_I, which governs the eventual decay of the conductivity, and (3) the mobility of positive charge ("holes" or "radical cation sites") along the polymer backbone, $\mu(h^+/P)$, which governs the absolute magnitude of the conductivity. All three parameters will depend to a greater or lesser extent on the length and the conformation of the polymer chains in solution. We begin therefore with a discussion of existing information relevant to these properties.

The weight-averaged molecular weight, M_w, of the MEH−PPV sample used, as determined by GPC using polystyrene standards, was ca. 600 kDa with a poly-dispersity index of ca. 3 corresponding to a number-averaged molecular weight, M_n, of ca. 200 kDa. The average number of monomer units per chain, $n = M_n/M_m$ with M_m the monomer molecular weight (260 g/mol), is therefore approximately 800 with a broad distribution around this number. If anything, the value of M_w, hence M_n and n, may be overestimates because of the more "rigid-rod" character of the PPV backbone compared with that of the polystyrene standards used. The value of $M_n = 200$ kDa was, however, consistently used to estimate the concentration of polymer chains in solution on the basis of the known weight per unit volume of MEH−PPV dissolved.

Aggregation of PPV derivatives in solution via $\pi-\pi$ interactions between different segments of the same chain or between separate polymer chains is a well known phenomenon which can lead ultimately to the formation of gels and solid precipitates. Even prior to phase separation, aggregation is usually apparent as a redshifted shoulder in the absorption band and a redshift in the fluorescence.[36−38] We have found no evidence for aggregation, in the form of redshifts in the absorption or emission bands, for benzene solutions of MEH−PPV up to the maximum concentration used in the present experiments, ca. 1 millimolar monomer units. Further support for the lack of aggregation has been provided by dynamic light-scattering measurements on *p*-xylene solutions of MEH−PPV which show the hydrodynamic radius of the polymer to be concentration independent up to monomer unit concentrations of 0.4 mM, the maximum investigated.[39] We conclude that the solutions studied in the present work consist of homogeneous suspensions of individual polymer chains free from inter- or intrachain $\pi\angle\pi$ interactions. Evidence that such interactions do ultimately occur at higher concentrations of MEH−PPV in chlorobenzene and tetrahydrofuran solvents has been presented in the form of a redshift in the photoluminescence excitation spectrum and a decrease in the effective hydrodynamic radius.[40] These effects are, however, only significant for concentrations that are an order of magnitude or more higher than the maximum used in the present work.

Because of the relatively large barrier of ca. 0.2 eV toward rotation out of an all-planar configuration of the phenylene−vinylene backbone,[9] PPV derivatives are expected to have properties characteristic of rigid-rod type polymers. This is confirmed by the long persistence lengths, from 10 up to more than 60 monomer units, determined by static light-scattering measurements on dilute solutions of dialkoxy-PPVs in *p*-

xylene.[39] As a result, individual polymer chains of MEH−PPV, with a (weight-averaged) molecular weight of ca. 600 kDa, have open structures with relatively large hydrodynamic radii, R_H, of 359, 215, and 125 Å in *p*-xylene, chlorobenzene, and tetrahydrofuran, respectively.[39,40] These values are to be compared with a radius of only ca. 40 Å expected for a compact spheroid of $M_n \approx 200$ kDa and density ca. 1 g/cm^3.

Since the molecular weight of the polymer used in the present work is similar to that in the dynamic light-scattering studies, we make the reasonable assumption that R_H will also be similar and close to the value of 359 Å determined in *p*-xylene, an aromatic solvent very similar to benzene.[39] This value of R_H corresponds to a diffusion coefficient of the polymer chains (via Brownian motion), D(P), of 1.0×10^{-7} cm^2/s, as given by the Stokes−Einstein equation,

$$D(\mathrm{P}) = \frac{k_B T}{6\pi\eta R_H} \tag{22}$$

with k_B the Boltzmann constant and η the viscosity of the solvent (0.65 cP for benzene). Assuming the chain conformation and hence the diffusion coefficient remain unchanged on abstraction of an electron, the mobility of the charged polymer chain as a whole, $\mu(P^+)$, can be estimated using eq 8 to be ca. 4×10^{-6} cm^2/Vs. This is more than 2 orders of magnitude lower than $\mu(Bz^+)$. Therefore, as mentioned previously, the *increase* in conductivity observed on transfer of charge from Bz^+ to a polymer chain can only be explained by the occurrence of rapid hole migration within the polymer agglomerate.

Because of the very open structure of the polymer chains, as evidenced by the large hydrodynamic radius and the lack of intrachain aggregation, the migration of holes will occur pseudo-one-dimensionally along the phenylene−vinylene backbone with a diffusion coefficient $D(h^+/P)$. The corresponding pseudo-one-dimensional, intrachain hole mobility is related to $D(h^+/P)$ via the Einstein relation,

$$\mu(h^+/P) = \frac{eD(h^+/P)}{k_B T} \tag{23}$$

Since the polymer backbone within an agglomerate as well as the agglomerates themselves will have a random orientation with respect to the electric field vector of the microwaves, the motion of the charge will be vectorially randomized. Therefore, the measured mobility will be an effective, isotropic value. The value of the mobility used in the fitting procedure was therefore taken to be $\mu(h^+/P)/3$.

The rate coefficient for the reaction of Bz^+ with the polymer, k_H, should be proportional to the sum of the diffusion coefficients of the reactants, that is, $[D(Bz^+) + D(P)]$. However, since D(P) is 2 orders of magnitude smaller than $D(Bz^+)$, k_H will be given to a good approximation by

$$k_H = 4\pi D(Bz^+) R_{eff}\left[1 + \frac{R_{eff}}{\sqrt{\pi D(Bz^+)t}}\right] \tag{24}$$

The form of eq 24, including the time-dependent term, has been taken to be the same as that derived for small reactants, eq 19, with however the "reaction radius", R_{ij}, replaced by an "effective reaction radius", R_{eff}. The validity of taking an equation of the form of eq 24 to be generally applicable even for large, nonspherical molecular entities is supported by the analytical expression derived by Traytak for a linear chain of n reactive moieties separated by a distance a each with a reaction radius

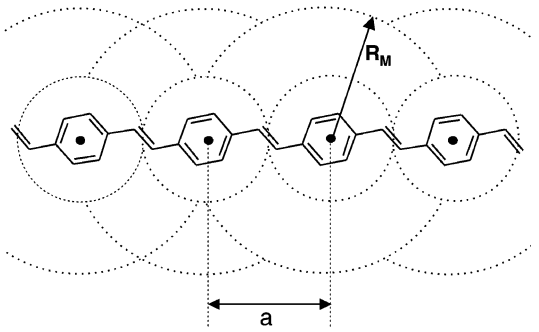

Figure 6. A short section of a phenylene−vinylene polymer modeled as a chain of reactive spherical sinks of reaction radius R_M and distance between the units a.

R_M as separate entities, see Figure 6.[17−19] In the Traytak solution, R_{eff} is given by

$$R_{eff} = \frac{nR_M}{1 + \frac{2R_M}{a}\ln n} \tag{25}$$

R_{eff} is clearly no longer a radius in the true sense of the word but is simply a length parameter.

In Figure 7A, we show attempted fits to the conductivity transient for a 1.25 μM PPV (1×10^{-3} mM PV monomer) solution using R_{eff} values in eq 24 of 40 Å (close to the radius of a compact sphere of molecular weight 200 kDa), 400 Å (close to the hydrodynamic radius, R_H), and 1000 Å (considerably larger than R_H). In all three cases, $D(Bz^+)$ was held constant at 3×10^{-5} cm^2/Vs and k_I and $\mu(h^+/P)$ were varied to obtain the best fit to the long time decay and the maximum value of the conductivity. For the three values of R_{eff} used, the best-fit values of k_I and $\mu(h^+/P)$ were 1.63 cm^2/Vs and 3.6×10^{11} M^{-1} s^{-1}, 0.42 cm^2/Vs and 1.2×10^{11} M^{-1} s^{-1}, and 0.46 cm^2/Vs and 1.2×10^{11} M^{-1} s^{-1}, respectively.

The fit to the experimental transient in Figure 7A, in the region of the after-pulse growth, is considerably better for $R_{eff} = 400$ Å than for either the smaller or larger values of R_{eff}. For $R_{eff} = 400$ Å and $D = 3 \times 10^{-5}$ cm^2/s, inequality (eq 21) indicates that the time-dependent term in k_H can only be neglected for times longer than ca. 2 μs. Since the growth of the conductivity occurs on a time scale much shorter than this, the time dependence of k_H plays an important role in the early time kinetics. The influence of the time-dependent term is illustrated in Figure 7B by the transient calculated using $R_{eff} = 400$ Å but neglecting the time-dependent term.

From fits to all of the transients shown in Figures 5 and 6, we have determined overall "best-fit" values for $\mu(h^+/P)$, k_I, and k_H of 0.46 cm^2/Vs, 1.2×10^{11} M^{-1} s^{-1}, and k_H given by eq 24 with $D(Bz^+) = 3 \times 10^{-5}$ cm^2/s and $R_{eff} = 360$ Å. The calculated curves shown in Figures 5 and 6 were obtained using these fixed values. The agreement with the experimental transients is reasonably good except for the highest dose pulse.

The value of $R_{eff} = 360$ Å for charge transfer from Bz^+ to MEH−PPV chains is very much larger than the 5−10 Å usually found for electron-transfer reactions involving relatively small molecular species. This is not particularly surprising since each of the ca. 800 phenylene−vinylene units comprising a polymer chain may be considered to be a potential reactive site. As mentioned above, an analytical solution for the rate coefficient for the reaction of a small reactant with a linear chain of n reactive moieties of individual reaction radius R_m and center-to-center separation distance a has been derived by Traytak.[17−19]

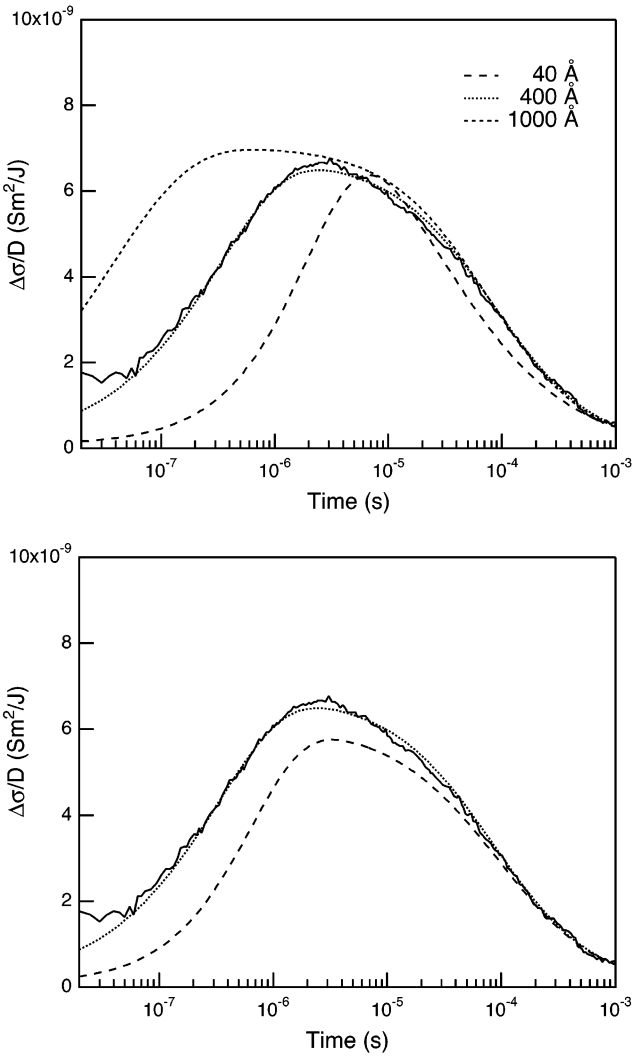

Figure 7. Full line: experimental conductivity transient on 10-ns pulsed irradiation of a 1.25 μM solution of MEH−PPV in benzene. Dashed lines: calculated kinetic fits in which the main variable is the effective reaction radius, R_{eff}, in eq 24 for the rate coefficient for charge transfer from Bz^+ to the polymer with $D(Bz^+) = 3 \times 10^{-5}$ cm^2/s. Figure 7B. Full line: experimental conductivity transient on 10-ns pulsed irradiation of a 1.25 μM solution of MEH−PPV in benzene. Dotted and dashed lines: calculated kinetic fits for $R_{eff} = 40$ nm and $D(Bz^+) = 3 \times 10^{-5}$ cm^2/s with and without the time-dependent term in the rate coefficient for charge transfer from Bz^+ to the polymer, eq 24, respectively.

The corresponding effective reaction radius for such a linear array is given by eq 25. Since R_M is expected to be similar in magnitude to half of the length of a PV unit (a/2), eq 25 can be approximated for large n by

$$R_{eff} \approx \frac{na}{2\ln n} \tag{26}$$

Substituting in eq 26 $a = 6.7$ Å (the actual length of a phenylene−vinylene unit) and $n = 800$, (determined by GPC and used in the fitting procedure), R_{eff} is estimated to be 401 Å, that is, close to the value of 360 Å found. As eq 26 shows, for large n the value of R_{eff} is (relatively) insensitive to the value taken for R_M. Using the full expression for R_{eff}, eq 25, with R_M values of a (6.7 Å) and a/2 (3.35 Å) results in R_{eff} values of 373 Å and 349 Å, respectively, which are even closer to the experimentally determined value. While a straight, linear array of reactive centers is without doubt an unrealistic representation of the much more complex three-dimensional structure of an MEH−PPV chain in solution, it does appear to provide a good description of the reaction kinetics using known quantities.

For comparison, we consider the effective reaction radius for a three-dimensional, cubic array of the reactive sinks with, as before, an individual reaction radius R_M and a center-to-center distance a between sinks. The solution derived by Traytak is[17]

$$R_{eff} = \frac{nR_M}{1 + \dfrac{2CR_M n^{(1-1/d)}}{a}} \tag{27}$$

with C a constant and d (=3) the dimensionality. The large n approximation of eq 27 is

$$R_{eff} \approx \frac{na}{2Cn^{(1-1/d)}} \tag{28}$$

Tseng et al.[41] have considered the "touching spheres" case, that is, $2R_m = a$, and have derived a value of $C = 0.80$ for diffusion-limited reaction with a cubic lattice. Taking $n = 800$ and $a = 6.7$ Å, which corresponds to a highly compact, globular structure, yields a value of $R_{eff} = 39$ Å. Using the full expression (eq 27) with R_M values of 3.35 Å and 6.7 Å results in no significant change in the value of R_{eff} calculated. Clearly, a highly compact structure is not capable of describing the reaction kinetics observed, as shown by the attempted fit using $R_{eff} =$ 40 Å in Figure 7A. This is not unexpected in view of the large value found for the hydrodynamic radius which indicates the polymer agglomerates have very open structures encompassing a volume several hundred times that expected for a compact sphere.

An open, three-dimensional structure can be simulated by allowing the cubic lattice parameter a in eq 27 and eq 28 to increase to values significantly larger than the individual reaction radius, that is, $a \gg 2R_M$. The value of a required to explain a given value of the effective reaction radius can then be determined from

$$a \approx \frac{2Cn^{(1-1/d)}R_{eff}}{n} \tag{29}$$

For $n = 800$, a value of $a = 62$ Å is required to explain the value of 360 Å for R_{eff}. Therefore, the average distance between reactive sinks needs to be approximately 10 times the distance between PV units along a polymer backbone to explain the kinetics observed.

For $a \gg 2R_M$ and large n, the length of a side of the cubic array, L, will be

$$L \approx a[n^{1/3} - 1] \tag{30}$$

For the above value of $a = 62$ Å, L is therefore 512 Å. The radius of a sphere with the same volume would be 318 Å which is quite close to the value of 359 Å for the hydrodynamic radius determined by light scattering. That there should be a close, quantitative relationship between the kinetic and hydrodynamic parameters of molecular clusters has previously been suggested by Tseng et al.[21,41]

Clearly, neither the simple linear chain nor the expanded cubic lattice are realistic representations of the actual MEH−PPV polymer chain conformation in dilute solution. The present kinetic results do, however, serve to confirm the conclusions from the light-scattering results of a very open structure with extensive, close-to-linear backbone segments. In this regard,

even the "best" PPV polymers invariably contain a few percent of chemical defects in the form of saturated (sp_3) and dehydrogenated (sp_1) vinylene moieties. Even a small percentage of such defects could have a controlling influence on the overall structure of a polymer agglomerate since they allow much more ready bending and twisting than the phenylene−vinylene backbone itself.[42,43]

Finally, we consider the value of the rate constant for charge recombination, k_I, which was taken to be time-independent of the basis of an expected reaction radius of 250 Å (R_C in benzene) and $[D(O_2^-) + D(P^+)] = 2.5 \times 10^{-5}$ cm^2/s. The time-dependent term in the recombination coefficient, according to eq 21, should therefore be negligible for times longer than ca. 1 μs. From the time scales of the transient decays, this condition is fulfilled for all but the highest dose pulse. The value of $k_I = 1.2 \times 10^{11}$ M^{-1} s^{-1} found is considerably smaller than the value of 4.7×10^{11} M^{-1} s^{-1} expected on the basis of $k_I = 4\pi R_c[D(O_2^-) + D(P^+)]$. The fact that the Debije relation does not provide a good estimate of k_I for this particular reaction is perhaps not surprising because the hydrodynamic radius of the polymer is in fact significantly larger than the Onsager escape distance: 360 Å versus 250 Å. The lower value of k_I could therefore be due to a substantially lower diffusion coefficient of O_2^- within the polymer agglomerate than in bulk benzene or to a lower effective reaction radius resulting from the one-dimensionally confined and possibly highly delocalized nature of the positive charge.

Summary and Conclusions

In this paper, we measure and discuss the kinetics of formation and decay of positively charged MEH−PPV polymer chains in pulse-irradiated benzene solutions. The progress of the reactions was monitored continuously as the change in the microwave conductivity of the solution over a time scale from nanoseconds to milliseconds using a single pulse. The kinetics of formation of MEH−PPV$^+$ by charge transfer from benzene radical cations occurs with an extremely large effective reaction radius, R_{eff}, of close to 400 Å. Because of this, the time-dependent term in the rate coefficient must be taken into account in the fitting procedure. The value of R_{eff} is in agreement with theoretical expectations for a linear chain of reactive sites of length equal to one phenylene−vinylene unit. Comparison with predictions for a hypothetical three-dimensional cubic lattice arrangement of the PV units indicates the polymer agglomerates have a very open, gel-like structure in agreement with the large hydrodynamic radius found in previous light-scattering measurements.

From the dependence of the decay kinetics of the conductivity on the initially generated ion concentration, we conclude that MEH−PPV$^+$ decays with a rate constant of 1.2×10^{11} M^{-1} s^{-1} by second-order recombination with O_2^- ions formed by electron attachment to oxygen. This rate constant is a factor of approximately 4 lower than expected for recombination according to the Debije equation which is most probably related to the fact that the hydrodynamic radius of the agglomerates (360 Å) is considerably larger than the Onsager distance in benzene (250 Å). No indication was found for a first-order component in the decay of the conductivity. Trapping of positive charge on the polymer chains (at chemical defect sites, for example) does not appear to occur within a time scale of several hundred microseconds at least.

The good agreement between the calculated and experimental conductivity transients for a range of polymer and initial charge carrier concentrations enables us to obtain an accurate value of 0.46 cm^2 V^{-1} s^{-1} for the pseudo-one-dimensional mobility of positive charge along isolated MEH−PPV chains in dilute solution.

Acknowledgment. The Priority Program for Materials research (PPM) of the Netherlands Organization for Scientific Research (NWO) is acknowledged for financial support.

References and Notes

(1) Conwell, E. M. In *Handbook of organic conductive molecules and polymers*; Nalwa, H. S., Ed.; John Wiley: New York, 1997; Vol. 4, pp 1−45.
(2) Drury, C. J.; Mutsaers, C. M. J.; Hart, C. M.; Matters, M.; de Leeuw, D. M. *Appl. Phys. Lett.* **1998**, *73*, 108−110.
(3) Friend, R. H.; Gymer, R. W.; Holmes, A. B.; Burroughes, J. H.; Marks, R. N.; Taliani, C.; Bradley, D. D. C.; Dos Santos, D. A.; Brédas, J.-L.; Löglund, M.; Salaneck, W. R. *Nature* **1999**, *397*, 121−128.
(4) Gelinck, G. H.; Geuns, T. C. T.; de Leeuw, D. M. *Appl. Phys. Lett.* **2000**, *77*, 1487−1489.
(5) Kraft, A.; Grimsdale, A. C.; Holmes, A. B. *Angew. Chem., Int. Ed.* **1998**, *37*, 402−428.
(6) Kraft, A. *ChemPhysChem* **2001**, *2*, 163−165.
(7) Grozema, F. C.; Siebbeles, L. D. A.; Warman, J. M.; Seki, S.; Tagawa, S.; Scherf, U. *Adv. Mater.* **2002**, *14*, 228−231.
(8) Hoofman, R. J. O. M.; de Haas, M. P.; Siebbeles, L. D. A.; Warman, J. M. *Nature* **1998**, *392*, 54−56.
(9) Grozema, F. C.; van Duijnen, P. T.; Berlin, Y. A.; Ratner, M. A.; Siebbeles, L. D. A. *J. Phys. Chem. B* **2002**, *106*, 7791−7795.
(10) Barzykin, A. V.; Seki, K.; Tachiya, M. *Adv. Colloid Interface Sci.* **2001**, *89*−*90*, 47−140.
(11) Murata, S.; Nishimura, M.; Matsuzaki, S. Y.; Tachiya, M. *Chem. Phys. Lett.* **1994**, *219*, 200−206.
(12) Van der Auweraer, M.; De Schryver, F. C. *Chem. Phys.* **1987**, *111*, 105−112.
(13) Kato, N.; Miyazaki, T.; Fueki, K.; Saito, A. *Int. J. Chem. Kinet.* **1988**, *20*, 877−884.
(14) Stroppolo, M. E.; Falconi, M.; Caccuri, A. M.; Desideri, A. *Cell. Mol. Life Sci.* **2001**, *58*, 1451−1460.
(15) Berezhkovskii, A. M.; Makhnovskii, Y. A.; Weiss, G. H. *J. Chem. Phys.* **2001**, *115*, 5376−5380.
(16) Smoluchowski, M. *Phys. Z.* **1916**, *17*, 557−571.
(17) Traytak, S. D. *Chem. Phys. Lett.* **1992**, *197*, 247−253.
(18) Traytak, S. D. *Chem. Phys. Lett.* **1994**, *227*, 180−186.
(19) Traytak, S. D. *Chem. Phys.* **1995**, *193*, 351−366.
(20) Lu, S.-Y.; Yen, Y.-M.; Tseng, C.-Y.; Tsao, H.-K. *J. Chem. Phys.* **2002**, *117*, 3431−3439.
(21) Tsao, H.-K.; Lu, S.-Y.; Tseng, C.-Y. *J. Chem. Phys.* **2001**, *115*, 3827−3833.
(22) Lee, S. B.; Kim, I. C.; Miller, C. A. *Phys. Rev. B* **1989**, *39*, 11833−11839.
(23) Gee, N.; Freeman, G. R. *Can. J. Chem.* **1992**, *70*, 1618−1622.
(24) Schmidt, W. F.; Allen, A. O. *J. Phys. Chem.* **1968**, *72*, 3730−3736.
(25) Gäumann, T.; Schuler, R. H. *J. Phys. Chem.* **1961**, *65*, 703−704.
(26) Infelta, P. R.; de Haas, M. P.; Warman, J. M. *Radiat. Phys. Chem.* **1977**, *10*, 353−365.
(27) Warman, J. M. In *The study of Fast Processes and Transient species by electron pulse radiolysis*; Baxendale, J. H., Busi, F., Eds.; Reidel: Dordrecht, The Netherlands, 1982; pp 433−533.
(28) Warman, J. M.; De Haas, M. P. In *Pulse Radiolysis*; Tabata, Y., Ed.; CRC Press: Boston, MA, 1991; pp 101−131.
(29) Shinsaka, K.; Freeman, G. R. *Can. J. Chem.* **1974**, *52*, 3495.
(30) Itoh, K.; Holroyd, R. *J. Phys. Chem.* **1990**, *94*, 8850−8854.
(31) Debye, P. *Trans. Electrochem. Soc.* **1942**, *82*, 265.
(32) Gelinck, G. H.; Warman, J. M. *Chem. Phys. Lett.* **1997**, *277*, 361−366.
(33) Warman, J. M. unpublished results.
(34) Allen, A. O.; de Haas, M. P.; Hummel, A. *J. Chem. Phys.* **1976**, *64*, 2587−2592.
(35) Warman, J. M.; Infelta, P. P.; De Haas, M. P.; Hummel, A. *Chem. Phys. Lett.* **1976**, *43*, 321−325.
(36) Gelinck, G. H.; Warman, J. M.; Staring, E. G. J. *J. Phys. Chem.* **1996**, *100*, 5485−5491.
(37) Gelinck, G. H. Thesis, Delft University of Technology, 1998.
(38) Gelinck, G. H.; Staring, E. G. J.; Hwang, D.-H.; Spencer, G. C. W.; Holmes, A. B.; Warman, J. M. *Synth. Met.* **1997**, *84*, 595−596.
(39) Gettinger, C. L.; Heeger, A. J.; Drake, J. M.; Pine, D. J. *J. Chem. Phys.* **1994**, *101*, 1673−1678.
(40) Nguyen, T.-Q.; Doan, V.; Schwartz, B. J. *J. Chem. Phys.* **1999**, *110*, 4068−4078.

(41) Tseng, C.-Y.; Tsao, H.-K. *J. Chem. Phys.* **2002**, *117*, 3448−3453.
(42) Hu, D.; Yu, J.; Wong, K.; Bagchi, B.; Rossky, P. J.; Barbara, P. F. *Nature* **2000**, *405*, 1030−1033.
(43) Candeias, L. P.; Grozema, F. C.; Padmanaban, G.; Ramakrishnan, S.; Siebbeles, L. D. A.; Warman, J. M. *J. Phys. Chem. B* **2002**, *107*, 1554−1558.